TALLINN UNIVERSITY OF TECHNOLOGY

Faculty of Science

Marine System Institute

THE IMPACT OF SURFACE CURRENTS AND SEA LEVEL ON THE WAVE FIELD EVOLUTION DURING ST. JUDE STORM IN THE EASTERN BALTIC SEA

Master's thesis

Marili Viitak

Supervisor: MSc. Ilja Maljutenko,

Tallinn University of Technology,

Institute of Marine Systems, Junior Researcher

Co-supervisor: PhD. Victor Alari,

Helmholtz-Zentrum Geesthacht,

Zentrum für Material- und Küstenforschung GmbH, Scientist

Earth Sciences

2015

Declaration

Hereby I declare that this master thesis, my original investigation and achievement, submitted for the master degree at Tallinn University of Technology has not been submitted for any academic degree. All content and ideas drawn directly or indirectly from external sources are indicated as such.

Marili Viitak

Supervisor: Ilja Maljutenko

Work meets the requirements for master's thesis.

The defence chief:

Accepted for defence of a thesis

....

(Name, signature, date)

TALLINNA TEHNIKAÜLIKOOL

Matemaatika-loodusteaduskond

Meresüsteemide instituut

PINNAHOOVUSTE JA VEETASEME MÕJU LAINEVÄLJA KUJUNEMISELE ST. JUDE TORMI AJAL LÄÄNEMERE IDAOSAS

Magistritöö

Marili Viitak

Juhendaja: MSc. Ilja Maljutenko,

Tallinna Tehnikaülikool,

Meresüsteemide Instituut, Nooremteadur

Kaasjuhendaja: PhD. Victor Alari

Helmholtz-Zentrum Geesthacht

Zentrum für Material- und Küstenforschung GmbH , Teadur

Maa-teadused

2015

TABLE OF CONTENTS

ABSTRACT

A third generation numerical wave model SWAN (Simulating WAves Nearshore) is used to study the impact of surface currents and sea level to wave field evolution.

The objective is to assess the surface currents and sea level effect on the wave field development and study the spatial variability.

For this purpose there is modelled a hindcast of a period 23.10.13 to 31.10.13. It includes a period of calm to moderate weather conditions and a storm named St. Jude. This period was chosen because during the storm the wind was blowing in the sector of S − SW (180-270^0) which is one of the most frequently occurring wind directions in the eastern Baltic Sea. Four runs with SWAN were made with different set-ups. First, reference run with dynamical forcing of wind. Second and third runs had dynamical forcings of wind and feedback of surface currents and sea level, respectively. Finally a run with all the dynamical forcings were taken into account. The input field of wind is obtained from atmospheric model HIRLAM; surface currents and sea level from circulation model HIROMB.

Results show clear effect of surface currents and sea level on the wave field evolution. It was seen in the increase and decrease of significant wave height. This was influenced by propagation directions of waves and surface currents and from the severity of conditions. Increase in the wave height was mostly seen in shallower waters and in areas where waves and surface currents were propagating in the opposite directions. In deeper parts of the eastern Baltic Sea and in case of waves and surface currents propagating in the same direction a decrease occurred.

Key words: SWAN, wave-current-water level interaction, coastal process, hindcast.

LÜHIKOKKUVÕTE

Kolmanda generatsiooni lainemudelit SWAN (Simulating WAves Nearshore) kasutati, et näha pinnahoovuste ja veetaseme mõju lainevälja kujunemisele.

Eesmärk oli hinnata pinnahoovuste ja veetaseme mõju lainevälja arengule ja uurida lainevälja ruumilist muutlikust.

Pidades silmas eesmärke, järelprognoos perioodist 23.10.13 – 31.10.13 modelleeriti kasutades SWANi. Periood hõlmab rahulikke ja mõõdukaid ilmastiku tingimusi ning tormi nimega St. Jude. Selline ajavahemik valiti seetõttu, et valdav tuule suund tormi ajal oli lõuna-lääne sektorist (180-270^0). See on ka üks kõige sagedamini esinev tuule suuna sektor Läänemere idaosas. Viidi läbi neli arvutust erinevate seadistustega. Esiteks, lähtearvutus, kus dünaamiliseks mõjuks oli tuul. Teisele ja kolmandale arvutusel olid mõjudeks tuul ning vastavalt pinnahoovused ja veetase. Viimasel arvutusel olid arvestatud kõi dünaamilised mõjud. Tuul pärineb imastiku mudelist HIRLAM. Pinnahoovused ja veetase tsirkulatsioonimudelist HIROMB.

Tulemused näitavad selget pinnahoovuste ja veetaseme mõju lainevälja kujunemisele. Seda oli näha olulise lainekõrguse kasvamisest ja kahanemisest. See oli mõjutatud laine ja pinnahoovuste levimis suundadest ja tingimuste tugevusest. Lainekõrguse kasvu oli näha madalama veetasemega piirkondades ning vastassuunalisel lainete ja pinnahoovuste levimisel. Läänemere sügavama veetasemega piirkondades ning lainetuse ja hoovuste samasuunalisel levimisel esines lainekõrguse kahanemine.

Märksõnad: SWAN, laine-hoovus-veetase, rannikuprotsessid, järelprognoos.

1. INTRODUCTION

Modelling, hindcasting and forecasting have a significant role in a wide range of activities connected to the marine environment. Sustainable coastal planning and development, safe ship navigation, water sports and all sorts of leisure pursuits are just a few of a long list. In case of storms and natural catastrophes, determining the risk level helps planning the evacuation. Therefore, it is possible to reduce human loss, damage on property, landscape and coastal ecosystems (Dietrich, *et al.,* 2013). In order to assess the risk, numerical models and forecasting systems come into play. Models are solving differential equations to see evolution of physical processes in the sea. In nature, everything is tightly connected and there is a feedback system between all the processes. More information about different interactions will give a better understanding of the sea.

The development of wave models from first generation models to third generation models, (e.g. SWAN (Booij, *et al.,* 1999), WAM (The WAMDI Group, 1988), WAVEWATCH (Tolman, 2009) has remarkably improved modelling accuracy of wave conditions. Same applies to circulation models (e.g. GETM (Burchard *et al.,* 2002), ADCIRC (Luettich *et al.,* 1992)) which are capable of modelling hydrodynamic and thermodynamic processes with great precision.

The ground work of wave-current interaction was done by Longuet-Higgins and Stewart in a series of papers (1960, 1961, 1964). They describe the interaction throughout the use of radiation stress and demonstrated the energy transfer between waves and currents. Bretherton and Gerrett (1968) introduced the idea of action

conservation. Since then numerous papers have been published including Wolf and Prandle, (1999), Soares (2006) ,van der Westhuysen (2012) and so on.

Alari (2013) studied the surge effect on wave field in the Baltic Sea. It showed that sea level deepening has an significant effect on wave field during extreme weather conditions. The effect of surface currents on wave field in the eastern Baltic Sea has had little attention. Therefore it is necessary to have more knowledge about this interaction.

The aim of the thesis is to improve the understanding of the physical processes and to see how wave field is affected by the surface currents and sea level in the eastern Baltic Sea. This will give information about where these interactions can be important during big storms. By studying the changes in space it will give information about potential measurements locations for waves and currents to take at the same time. This will help in the future to improve modelling systems and to see if it is worth further on to investigate coupling of wave and hydrodynamic models in the Baltic Sea.

Present study has two mean objectives. Firstly, to assess the one-way interaction between waves, surface currents and sea level in almost tideless (up to 10 cm (Feistel *et al*., 2008)) coastal area. It will try to answer a questions: how surface currents and sea level effect significant wave height? Secondly, to study the spatial variability of surface currents and sea level effect on wave field. For this purpose simulation of wave field with wave model SWAN is conducted and also compared to measurements.

Thesis is structured as follows. In chapter 2 a theory of wave, surface currents and sea level interaction is presented. It is followed by the description of SWAN wave model in chapter 3. In chapter 4 data and methods used in the study are described. Results and discussion are in chapter 5. Conclusion is in chapter 6.

2. WAVE, SURFACE CURRENTS AND SEA LEVEL INTERACTIONS

The purpose of this chapter is to give a literature overview of the topic. Describing the theoretical background of surface currents and sea level effect on waves.

2.1 Magnitude of significance' of processes in coastal waters

In deep waters (water depth greater or equal than half of the wavelength) and coastal waters (depth smaller than half of the wavelength) different processes are relevant in shaping the wave field.

In coastal areas, the bottom starts by affecting the wave field, which has no effect in deep waters. In Battjes (1994) there has been compared different physical processes that have an impact on development of the waves and their relative importance in oceanic and coastal waters. It was brought out that the evolution of waves in coastal waters is impacted with various processes that could be neglected in deep waters. In near-shore bottom friction, current refraction, energy bunching, bottom refraction, shoaling, breaking, triad wave-wave interactions and reflection becomes significant.

To estimate the wave field characteristics accurately, more detailed knowledge about these processes is necessary. Waves, surface currents and sea level interaction are a complex feedback system where each one has an impact to the other. The thesis concentrates on one part. How wave field is influenced by surface currents

and sea level.

In the next section surface currents and sea level effect on waves are described.

2.2 Surface currents and sea level effect on waves

Interaction between waves, surface current and sea level lead to changes in generation, propagation and dissipation mechanism of waves.

Changes in the sea level influences bottom friction, refraction, shoaling and depth-induced breaking. In general it affects mostly wave propagation and dissipation (Holthuijsen, 2007).

Surface currents influence all three aspects of waves, generation, propagation and dissipation (Jonsson, 1990).

2.2.1 Wave generation

In practice, the energy input to the wave model determines the correct rate of wave growth (Holthuijsen, 2007). Growth of wind waves starts with pressure fluctuations carried along by the mean wind. When the wind reaches to a certain threshold velocity capillary waves develop on the water surface. When wind continues to blow over the surface of the water waves grow and start to affect also the air flow. With increase in surface roughens the transfer of energy from the wind enhance (Thomson, 1981).

Surface currents dynamic effect on waves include so-called wave age effect. Wave field travelling in ambient opposing current will have lower effective wave age. In other words wave tend to break faster. One option to define the wave age β is the ratio of wave phase speed c and wind speed U_{10} at 10-m above sea surface (Liu

et al., 2007)

$$\beta = \frac{c}{U_{10}} \tag{1}$$

Lower effective wave age implies to a younger wind sea state. Waves have a short period and high frequency. Coupling between wind and waves is stronger compare to the old wind sea. Therefore, resulting in stronger momentum transfer from the wind. For following current the effect is reversed (Van der Westhuysen, 2012).

2.2.2 Wave propagation

Surface currents and sea level induce changes in the wavelength, height and direction due to changes in the phase speed and therefore in the group velocity (Holthuijsen, 2007).

Shoaling

Waves can be described with dispersion relationship

$$\omega^2 = g\,k\,\tanh(kd) \tag{2}$$

where ω^2 is the square of radian frequency, *g* acceleration to due the gravity, k is wave number and d water depth. A wave propagating over a fixed seabed with gentle slope will retain its frequency. As the waves enter to a shallower water dispersion relationship (eq. 2) will stay valid and changes in the group velocity occur. Group velocity c_g can be calculated as,

$$c_g = nc \quad \text{with} \quad n = \frac{1}{2}\left(1 + \frac{2\,kd}{\sinh(2\,kd)}\right) \tag{3}$$

where *k* is wave number and *d* water depth. Waves travelling across the water surface carry their potential and kinetic energy with them. Group velocity is the velocity of local wave-energy transport normal to the wave crest P_{energy}

12

$$P_{energy} = E\,c_g \quad \text{with} \quad E = \frac{1}{2}\rho g a^2 \tag{4}$$

where E is the wave energy, ρ is water density and a^2 is the square of the amplitude of the wave. Therefore, changes in the group velocity cause changes in wave energy transport (i.e. in kinetic and potential energy). In order to maintain constant flux of kinetic and potential energy (in a closed/stationary system) decrease in the energy transport must be compensated by an increase in the energy density. This results in an increase in wave height and phenomena is called shoaling, also "energy bunching. In other words, with shoaling compacting of horizontal wave energy takes place (Holthuijsen, 2007).

The kinematic effects of uniform surface currents on wave propagation include changes in wave phase velocity and wave number. The absolute wave group velocity c_a will be shifted away from the relative phase speed c_r by the current component c_c in the wave direction so that,

$$c_a = c_r + c_c \tag{5}$$

If waves enter a region with opposing current increasing in strength (e. g. negative current gradient) waves become shorter and steeper. That implies that wavelength will be shortened and wave number will increase. Opposing current has similar effect on waves as depth-induced shoaling. In the opposite case, entering a region with following current increasing in strength (e. g. positive current gradient), waves become longer and less steep. Therefore wavelength will be lengthened and wave number will decrease (Phillips, 1977). The experiment conducted by MacIver *et al.* (2006) confirm this kind of behaviour of waves.

The high frequency part of waves is more affected of current shoaling than low frequency (Holthuijsen, 2007).

Depth-induced refraction

Depth-induced refraction turns the crests of the waves more parallel to the shore (Wolf and Prandle, 1999). This is due to the changes in the phase speed along the wave crest. Phase speed *c* can be calculated as

$$c=\sqrt{\frac{g}{k}\tanh(kd)} \tag{6}$$

As an example the wave travelling in the direction of n-axis can be looked (see fig. 1). If the phase speed is increasing in positive direction of m-axis then wave crest turns more to the right. Waves are always turning to a region where the propagation speed is lower i.e. toward shallower water. This is also resulting in an increase or decrease in the wave height depending on the actual changes in wave direction (Holthuijsen, 2007).
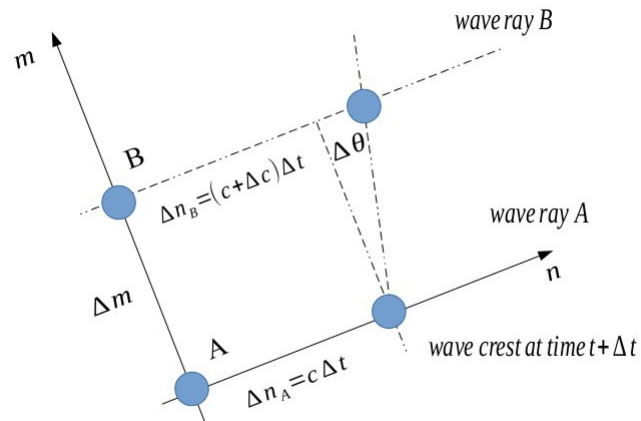
Figure 1. This is a figure of refraction scheme. In the counter-clockwise system with m-and n-axis. m-axis following wave crest and n-axis wave rays. Two point A and B on a wave crest at time t will travel a distance $\Delta n_A = c\Delta t$ $\Delta n_B = (c+\Delta c)\Delta t$, c being the phase speed. If Δc is positive and increasing in the direction of m than waves turn more to the right e.g. $\Delta\theta$ will be negative (Holthuijsen, 2007).

Surface current induced refraction

When waves encounter a current gradient obliquely, current induced refraction occurs. Currents effect on wave propagation, compare to depth, is more subtle. The current refraction causes waves to turn towards the direction of the current axis and it depends on the gradient and spatial variation of the current (Wolf and Prandle, 1999). In case of opposing shared current, waves will be refracted in the direction of decreasing current velocity. with following current, in the direction of increasing current velocity (Haus, 2007). Nwogu (1993) was the first to conduce an experimental and theoretical study to see the effects of steady currents on wave spectra directional spreading. The study showed that whenever the current speed was negative, there was a cut-off frequency in the energy density and relative importance of currents was vivid in high wave number or frequency range of the spectrum compared to low.

Wave blocking

Additionally, with opposing current, waves can get blocked. This happens when the current is strong enough to stop the wave travelling upstream. At that point the current velocity and wave relative velocity becomes equal (i.e. wave speed is zero relative to current speed) and just before that waves get very steep. This may cause navigation hazards. After the blocking point waves can break or be reflected. This has been studied by Chawla and Kirby (1998).

2.2.3 Wave dissipation

Depth-induced breaking

Wave breaking is largely caused by depth-induced breaking. The average energy loss can be calculated as,

$$D'_{surf} = \frac{-1}{4} \alpha_{BJ} Q_b f'_0 H^2_{max} \qquad (7)$$

where $\alpha_{BJ} \approx 1$ is a tunable coefficient, Q_b the friction of breaking waves, f'_0 is the mean zero-crossing frequency of the breaking waves and H^2_{max} is a square of the maximum wave height, below that waves do not break.

$$H_{max} = \gamma (d + \acute{\eta}) \qquad (8)$$

is a function of breaking index (γ), local water depth d and wave-induced set-up $(\acute{\eta})$. From eq. 7-8 it can be see that sea level changes play an important role in determining the breaking waves rate (Ris and Holthuijsen, 1996).

Current induced breaking

In the presence of currents enhanced wave dissipation has been noticed. As the shape and behaviour of the waves changes in the presence of currents, also some modifications and additional physical processes occur. In case of a wave travelling on an opposite current, the transfer of energy from currents to waves can only last to a certain limit. At one point it will be impossible for the waves to grow any bigger and the waves will break. The breaking of waves is faster with absence of opposing surface currents. with following current the wave dissipation rate decreases, because current stretches a wave to be longer. This has been studied by Ris and Holthuijsen (1996) and van der Westhuysen (2012).

Wave-current induced bottom dissipation

Wave-current interaction in the bottom boundary layer results in larger friction coefficient in a current regime than with no currents (Wolf and Prandle, 1999). This thesis concentrates on interactions in horizontal dimension. For more information on wave-current interaction in vertical dimension see e.g. Soulsby *et al.*, (1993) and Rosales *et al.*, (2008).

Change in the energy spectrum

As there is an exchange of energy between waves and currents (Lonquet-Higgins and Stewart, 1964, 1960, 1961, 1962), the spectrum of the wave energy is modified. The free surface spectral energy will increase with an opposite current and decrease with following current. Also, the differences are bigger when waves are smaller and currents stronger (Soares and de Pablo, 2006). Huang *et al.*, (1972) were the first to present an equation that described the changes in the wave spectral shape in the present of currents. As the phase speed *c*, frequency ω and wave number k of a gravity wave are related as following

$$c = \frac{\omega}{k} \qquad (9)$$

The phase speed is a monotonically decreasing function, so at higher wave number the influence of currents will be predominant. wave number is defined as density of the waves, that is, the number of wave crests per unit length (Holthuijsen, 2007),

$$k = \frac{2\pi}{\lambda} \qquad (10)$$

All of the above described effects of surface currents and sea level on waves are summarized in a table 1 in the next bage.

Table 1. Effects of currents and sea level on waves.

	Currents		Sea level
	Opposing current	Following current	
Wave generation			
Wave age	Lower effective wave age ↓ Stronger momentum transfer from wind	Higher effective wave age ↓ Weaker momentum transfer from wind	
Wave propagation			
Depth-induced shoaling			Depth-induced changes in group velocity ↓ Increase in wave height
Wave group velocity	Absolute group velocity will be shifted away from the relative phase speed by the current component		Group velocity decreases proportionally to depth
Wave height	Increases	Decreases	
Wavelength	Decreases	Increases	
Wave steepness	Increases	Decreases	
Wave number	Increases	Decreases	
Refraction	Current-induced changes in the phase speed ↓ Change in the wave direction (turn toward current axis, in the direction of decreasing current speed)	Current-induced changes in the phase speed ↓ Change in the wave direction (turn toward current axis, in the direction of increasing current speed)	Depth-induced changes in the phase speed ↓ Change in the wave direction (mean wave direction towards shore normal)

Wave blocking	Just before current and wave relative velocity become equal ↓ Wave height increases rapidly ↓ current and wave relative velocity are equal ↓ Waves get blocked	
Wave dissipation		
Wave breaking	Enhanced breaking of waves	Depth-induces breaking
Bottom dissipation	Wave-current interaction increases bottom friction coefficient	In shallower waters bottom friction coefficient increases
Wave spectral energy density	Increases Decreases	

3. NUMERICAL MODEL

In the present study wave model SWAN is used for modelling the wave field. The following provides the description of the model.

3.1 SWAN - Simulating WAves Nearshore

SWAN is third-generation numerical wave model developed by Delft University of Technology, in Netherlands. Waves are described with the two-dimensional wave action density spectrum (Booij and Holthuijsen, 1999). The action density spectrum N is considered instead of the energy density spectrum E because in the presence of ambient currents, action density is conserved but energy density is not. Action density is proportional to energy density (Whitman, 1974),

$$N(\sigma,\theta)=\frac{E(\sigma,\theta)}{\sigma} \tag{11}$$

The variable σ is the relative frequency (as observed in a frame of reference moving with the current velocity) and θ is the wave direction (the direction normal to the wave crest of each spectral component). SWAN model solve the spectral action balance equation without any *a priori* restrictions on the spectrum for the evolution of wave growth (Booij and Holthuijsen, 1999). The action balance equation in Cartesian coordinates:

$$\underbrace{\frac{\partial N}{\partial t}}_{\text{I}}+\underbrace{(\vec{c_g}+\vec{U})\nabla_{x,y}N}_{\text{II}}+\underbrace{\frac{\partial c_\sigma N}{\partial \sigma}}_{\text{III}}+\underbrace{\frac{\partial c_\theta N}{\partial \theta}}_{\text{IV}}=\frac{S_{wind}+S_{nl3}+S_{nl4}+S_{wc}+S_{bot}+S_{db}}{\sigma} \tag{12}$$

On the left-hand side of equation (12) the first term (I) represents the local rate of change of action density in time; the second term (II) denotes the propagation of wave energy in two dimensional geographical space, where $\vec{c}_g$ is the group velocity and $\vec{U}$ the ambient current. The third term (III) represents shifting of the relative frequency due to variations in depths and currents (with propagation velocity c_σ in σ space). The fourth term (IV) represents depth induced and current-induced refraction (with propagation velocity c_θ in θ space). At the right-hand side of the action balance equation is the source term that represents all physical processes which generate, dissipate, or redistribute wave energy. These terms denote, respectively, wave growth by the wind S_{wind}, non-linear transfer of wave energy through three-wave S_{nl3} and four-wave interactions S_{nl4} and wave dissipation due to whitecapping S_{wc}, bottom friction S_{bot} and depth-induced wave breaking S_{db} (The SWAN team, 2013a).

3.2 SWAN - accounting currents and sea level

This chapter describes how currents and sea level has been implemented in the SWAN wave model.

SWAN itself is not capable to calculate surface currents and sea levels. In order to take them into into account they have to to be presented as input. If there is no data, these terms are equal to zero (The SWAN team, 2013b).

3.2.1 Wind

Two mechanism are used to describe the transfer of wind energy resonance mechanism (A) and a feed-back mechanism (B) . For more precise description see Phillips (1957) and Miles (1957).Wave growth is a sum of linear (A) and exponential (B) growth

$$S_{wind}(\sigma,\theta)=A+BE(\sigma,\theta) \tag{13}$$

in which A and B depend on wave frequency and direction, and wind speed and direction. Linear wave growth (A) contributes to the initial stages of wave growth. As the waves grow they start to effect the wind induced pressure field, which results in a larger energy transfer from the wind as the waves grow. To account the currents the apparent local wind speed and directions are used (The SWAN team, 2013a).

As it was described in section 2.2.1 *Wave age effect*. In the presence of surface currents travelling opposite to the wave direction the transfer of wind energy to the waves is stronger and vice versa.

3.2.2 Kinematic effects

On equation (12) the kinematic effects are presented with terms II, III and IV. As it was stated in Whitman, (1974), wave energy propagation velocities in spatial and spectral space can be described by the kinematics of a wave train:

in spatial space

$$\vec{c}_g+\vec{U}=\frac{1}{2}\left(1+\frac{2|\vec{k}|d}{\sinh(2|\vec{k}|d)}\right)\frac{\sigma\vec{k}}{|\vec{k}|^2}+\vec{U} \tag{14}$$

c_g is group velocity vector; $\vec{U}=(u_x,u_y)$ is ambient current velocity vector; $\vec{k}=(k_x k_y)=(|\vec{k}|\cos\theta,|\vec{k}|\sin\theta)$ is wave number vector; d is the total water depth and σ relative frequency.

In spectral space

$$c_\sigma=\frac{\partial\sigma}{\partial d}\left(\frac{\partial d}{\partial t}+\vec{u}\,\nabla_{x,y}d\right)-c_g\vec{k}\frac{\partial\vec{u}}{\partial s} \tag{15}$$

$$c_\theta=\frac{-1}{k}\left(\frac{\partial\sigma}{\partial d}\frac{\partial d}{\partial m}+\vec{k}\frac{\partial\vec{u}}{\partial m}\right) \tag{16}$$

c_σ, c_θ are the propagation velocities in spectral space σ-,θ-space; s is space coordinate in the wave propagation direction of θ and m is a coordinate

22

perpendicular to *s* (The SWAN team, 2013a).

From kinematics in spatial space and spectral space (eq.14 and 15) it is seen, when waves and currents are propagating in the opposite directions, term II will get a smaller value in eq. 12. This will result with an increase in the wave energy (see eq. 11) and therefore also in the wave height. With waves and currents propagating in the same direction the effect is reversed.

As the sea level changes the total water depth influences the height of the waves. The group velocity will start to decrease proportionally to the water depth (eq. 3). To maintain a constant flux of energy transport an increase in the energy density occurs. This results in an increase of the wave height (see section 2.2.2 *Shoaling*).

With varying surface current and sea level refraction occurs (eq. 16). For more detailed description see section 2.2.2, *Depth induced refraction* and *Current induced refraction)*.

Shoaling and refraction are represented in eq.12 with terms II, III and IV.

3.2.3 Depth-induced wave breaking

Sea level will determine the height of the waves after which the waves will start to break (see section 2.2.4 *Depth induced breaking*).

Energy dissipation due to the depth-induced wave breaking is bore based model applied to random waves (Battjes and Jansen, 1978)

$$S_{db}(\sigma,\theta) = \frac{D_{tot}}{E_{tot}} E(\sigma,\theta) \tag{17}$$

$D_{tot} = -\alpha_{BJ} Q_b \widetilde{\sigma} H_{max}^2 (8\pi)^{-1}$ is the mean rate of energy dissipation per unit horizontal area due to wave breaking. $\alpha_{BJ} = 1$, Q_b is the fraction of breaking waves. $H_{max}^2 = \gamma d$ is the maximum wave height that can exist at the given where γ is the breaker parameter and d total water depth. E_{tot} is the total wave energy integrated over all directions and frequencies (The SWAN team, 2013a).

23

3.2.4 Whitecapping

In the presence of currents waves are experiencing enchant whitecapping (see section 2.2.3 *Current induced breaking*).

Whitecapping is represented by the pulse-based model of Hasselmann (1974)

$$S_{wc}(\sigma,\theta) = -\Gamma \widetilde{\sigma} \frac{k}{\widetilde{k}} E(\sigma,\theta) \tag{18}$$

where $\widetilde{\sigma}$ denote the mean frequency and $\widetilde{k}$ the mean wave number. The coefficient Γ depends on the overall wave steepness (The SWAN team, 2013a). With opposing current the energy density will increase also the wave number and wave steepness increase.

3.2.5 Bottom friction

Empirical model of JONSWAP (Hasselmann *et al.,* 1973) is used to express bottom friction

$$S_{bot} = -C_b \frac{\sigma^2}{g^2 \sinh^2(kd)} E(\sigma,\theta) \tag{19}$$

where $C_b = C_{JON} = 0.038$ m^2 s^{-3} bottom friction coefficient (The SWAN team, 2013a).

As the surface currents are affecting the spectral wave energy also the bottom friction will experience change. Bottom friction will increase with increasing wave energy e.g. in case of a opposite current (see section 2.2.3 *Wave-current induced bottom dissipation*).

4. DATA AND METHODS

4.1 Investigation area

The investigation area is the eastern Baltic Sea, which is shown on fig. 2. It includes two gulfs – Gulf of Finland and Gulf of Riga. Depth varies between 0 to 170 meters.

Gulf of Finland is connected with Baltic Proper without having any limiting condition for the propagation of the waves which allows in under certain meteorological conditions long and high waves to enter the region. According to Kahma and Petterson (1993) the mean significant wave height in spring is 0.5 m with peak period of 3,8 s and in winter 1.3 m with period of 5,3 s. Higher waves are produced in storm conditions (Soomere *et al.,* 2008).

In Gulf of Riga the wave propagation and growth are limited by shallow and narrow straits. Annual average wave height is between 0,25 – 0,5 m (Suursaar *et al.,* 2012). According to Raudsepp, *et al.* (2011) the peak period ranges between 2,3 – 8 s.

On fig. 2 red and black squares show the stations were the measurement were taken (see section 5.1 Validation) to compare with the model runs.
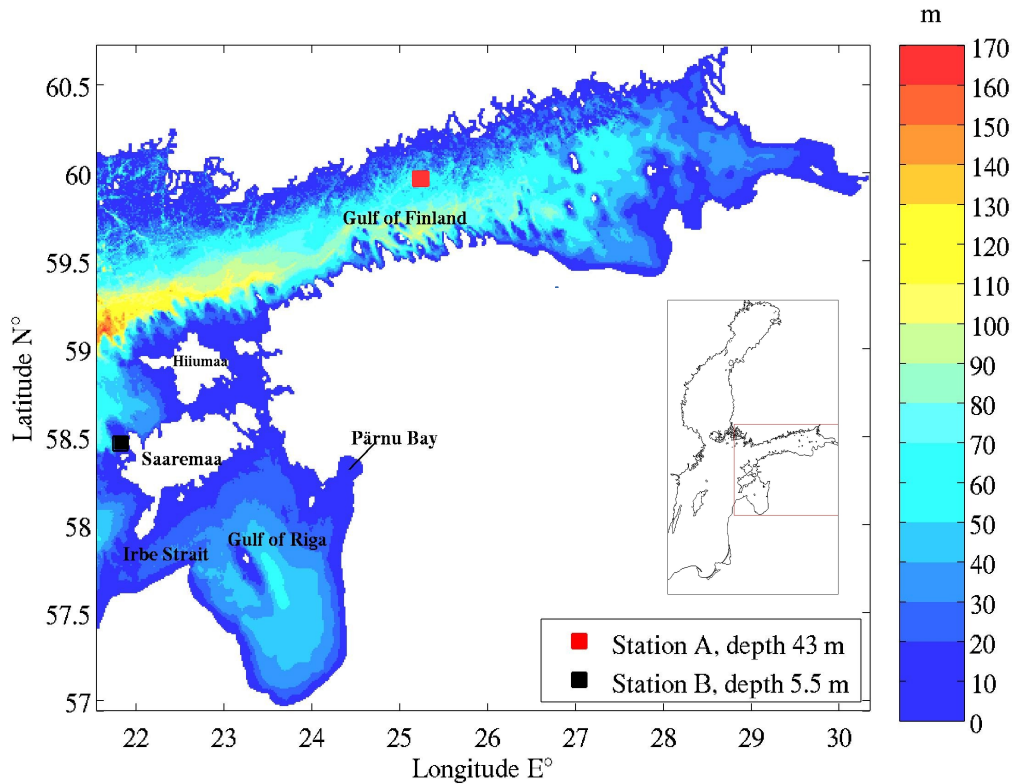
Figure 2. This is a figure of the eastern Baltic Sea bathymetry with grid resolution of 0.5 nautical miles. On the right side if the figure there is the displayed the Baltic Sea contour with red square showing the eastern Baltic Sea area.

4.2 Model set-up and dynamical forcing

For modelling with SWAN nesting approach was used. The whole Baltic Sea region was simulated with resolution of 1 nautical miles. From there boundary conditions were obtained for the eastern Baltic Sea, which had a resolution of 0.5 nautical miles. Contour of the area is shown on fig. 2, right side.

SWAN was forced with wind field interpolated to HIROMB (Funkquist and Kleine, 2007) computation grid from atmospheric model HIRLAM (Unden e*t al.*, 2002). HIRLAM wind fields were with resolution 11 km. This resolution was used to interpolate to 1 and also for 0.5 nautical miles grid. Additionally input of surface

currents and sea level were taken from HIROMB. SWAN computational grid and HIROMB grid are identical in order to avoid interpolation errors.

For bathymetry the Baltic Sea Bathymetry Database data was used (Baltic Sea Hydrographic Commission, 2013). This was interpolated to SWAN computational grid which was identical to HIROMB grid.

Time step for SWAN runs was 10 minutes with directional spreading of 10 degrees. Input fields of wind, currents and sea level to the wave model had a time step of 1 hour. Output of SWAN was requested in every 1 hour. Current values for 1 nautical mile grid were taken from 4 m depth from the surface. For 0.5 nm grid the depth was 3 m. This is a peculiarity of HIROMB. As the closest current velocities to the surface were in depth 3m therefore in the thesis surface currents are refer to as the currents in depth of 3 m.

Four model runs with SWAN were made using different dynamical forcings. There was considered wind, surface currents and sea level. On table 2 there is a description of all the runs. Firstly, reference run with SWAN where there was only forcing of wind. On the second run, additionally to the wind, surface currents were included. with third run, wind and sea level impact was taken into account. Finally, in fourth run, all the dynamical forcings were present.

Table 2. Description of SWAN runs.

r1 - run1	reference, wind
r2 - run 2	wind and surface currents
r3- run 3	wind and sea level
r4 - run 4	wind, surface currents and sea level

It is assumed that the current and sea level are not affected by the wave field.

4.3 Modelling period and weather conditions

For modelling 9 days period was chosen, from 23.10.2013 to 31.10.2013. This includes calm to moderate weather conditions and a storm.

A time series of HIRLAM wind speed near west coast of Saaremaa in measurement station B (see fig. 2) is shown on fig. 3.
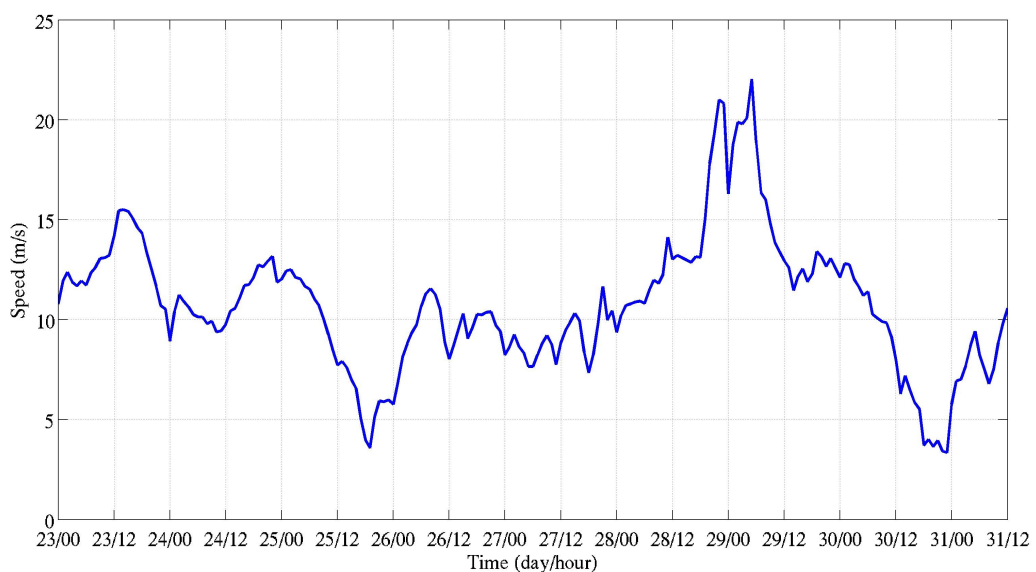
Figure 3. This is a figure of time series of HIRLAM wind speed in in station B from modelling period 23.10.2013 – 31.10.2013

Form 23.10 to 28.10 wind speed ranges between 4 – 15 m s^{-1} which is considered to be calm to moderate weather. The storm, named St. Jude, lasted three days. It arrived to Estonia in the evening of 28.10 and reached the highpoint on 29.10 early morning. Weather starts to calms down in the beginning of next day.

At the highpoint of the storm, in 29.10.13 at 04.00 wind speed, current velocity, sea level and significant wave height are shown on figures 4, 5,6 and 7.

On fig. 4 there is a snapshot of wind speed and direction on the morning of 29.10

at 04.00.
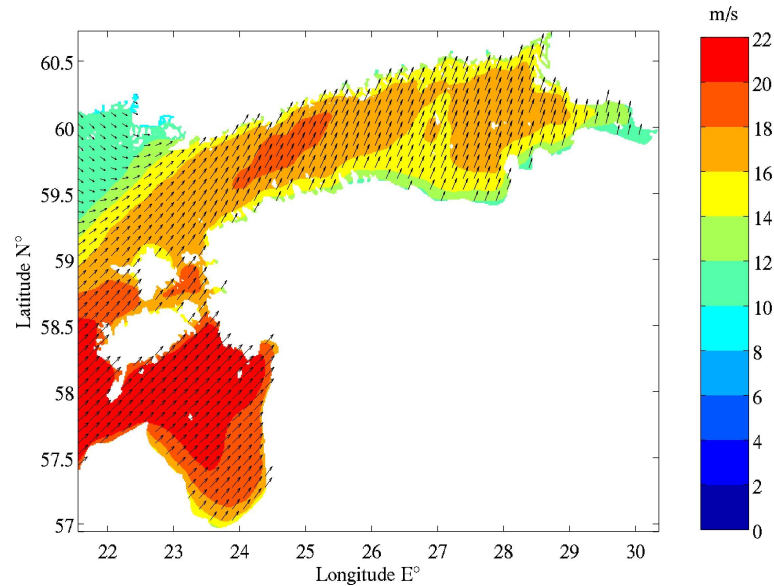
Figure 4. This is a figure of wind speed and direction on 29.10.13 at 04.00

During a storm wind speed reaches up to 22 m s^{-1}. It was blowing from the sector S − SW which is also one of the most frequent wind direction in the Baltic Sea (Jaagus and Kull, 2011).

On fig. 5 it can be seen surface current velocities and propagation direction (every 10th vector is displayed) at the highpoint of the storm. Velocity reaches up to 195 cm s^{-1} in the Irbe strait. In Gulf of Finland, in Pärnu bay and around Hiiumaa and Saaremaa the highest values are up to 90 cm s^{-1}. Near the shore, surface currents are strongly affected by the coast line. As the wave crests start to turn more parallel to the shore the propagation angle between surface currents and waves increase. Therefore an increase in the wave height is expected near the shore.

29
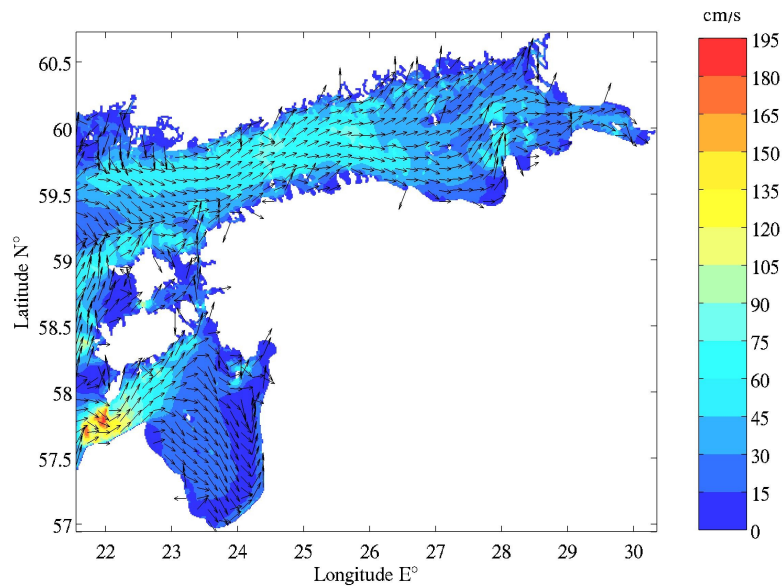
Figure 5. This is a figure of current velocity and direction on 29.10.13 at 04.00

On fig. 6 difference from the mean sea level in Pärnu bay was up to 200 cm. In south east of Hiiumaa and Saaremaa, Finnish coast and Irbe strait there was a difference up to to 80 cm. In the deeper parts of eastern Baltic it ranges from 80 to 100 cm.
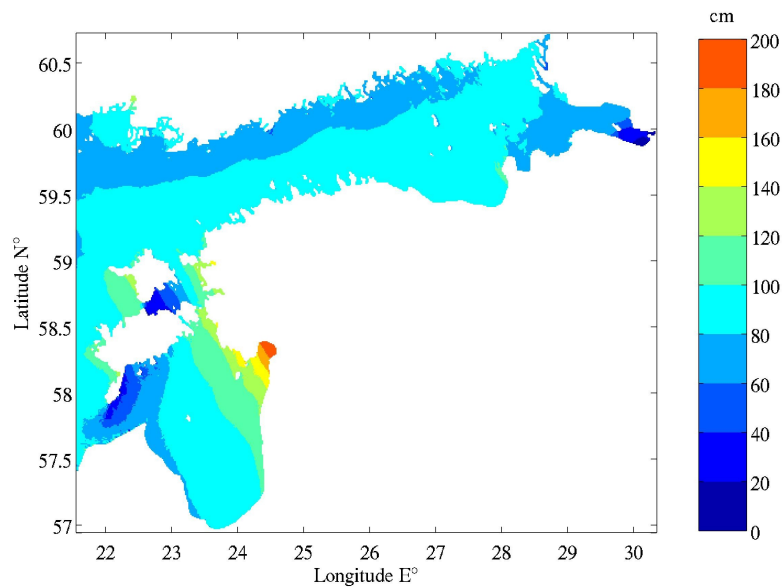
Figure 6. This is a figure of the increase in the sea level on 29.10.13 at 04.00.

Significant wave height on fig. 7 is 6.5 m in the western part of the eastern Baltic Sea. Entering the Gulf of Finland and Gulf of Riga the wave height starts to decrease. Near the shore it is as big as 2 to 2.5 m.
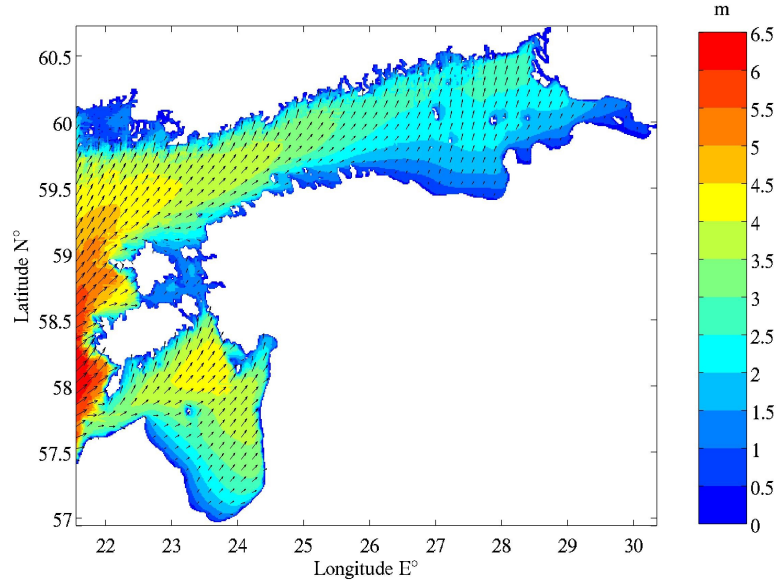
Figure 7. This is a figure of significant wave height on 29.10.13 at 04.00.

4.4 Wave parameters and statistics

To see the changes in the wave field significant wave height (Hs) which is the mean of 1/3 of the highest waves. In SWAN it is expressed as,

$$Hs = 4\sqrt{\iint E(\omega, \theta)\, d\omega\, d\theta} \tag{20}$$

where $E(\omega, \theta)$ is the energy density spectrum.

Modelling results were compared to wave measurement. To evaluate the consistencey of measurements and model four statistical parameter were calculated: root mean square error (RMSE), scatter index, BIAS and correlation coefficient.

$$RMSE = \sqrt{\frac{1}{n}\sum_{i=1}^{n}(a_i - b_i)^2} \tag{21}$$

31

$$scatter\ index = \frac{RMSE}{\frac{1}{n}\sum_{i=1}^{n} b_i} * 100 \qquad (22)$$

$$BIAS = \frac{\sum_{i=1}^{n} (a_i - b_i)}{n} \qquad (23)$$

where a is the model data, b is the measurement and n the number of elements.

In order to see effects of different dynamical forcings a significant wave height changes were studied by comparing significant wave height $\Delta Hs^n(t)$ of each model run ($n=2,3,4$) with reference run n=1 (eq. 26). To see the maximum range of possible change in significant wave height the maximum difference in the time period of the storm day 29.10.13 was calculate. The maximum difference $\Delta m Hs^n$ for each grid point (x, y) was found as

$$\Delta m Hs^n = \Delta Hs^n(t_{max}^n) \quad . \qquad (24)$$

Where t_{max}^n (eq. 25) is the time when the difference of significant wave height (eq. 26) is maximum.

$$t_{max}^n = arg\,max\left(|\Delta Hs^n(t)|\right) \qquad (25)$$

$$\Delta Hs^n(t) = Hs^n(t) - Hs^1(t) \qquad (26)$$

And the relative change

$$\Delta r Hs^n = \frac{\Delta m Hs^n}{Hs^1} * 100 \qquad (27)$$

$$Hs^1 = Hs^1(t_{max}^n) \qquad (28)$$

where the significant wave height of reference run r1 Hs^1 was found at time moment t_{max}^n .

5. RESULTS AND DISCUSSION

5.1 Validation

First model runs are compared with measurements taken in deep water (depth 43 m) and close to the shore (depth 21 m) (measurement station A and B in fig. 2, respectively).

The time period for the validation in deep water is from 23.10.13 to 31.10.12. Measurements were taken in Gulf of Finland (fig. 2, station A) by Finnish Meteorological Institute (FMI). Device used was WAVERIDER MKIII which registers surface acceleration. Data was registered with time step of 1 hour and waves with period of 1.6 s and higher.

On fig. 8, in the next page, significant wave height of the run r1 to r4 are compared to measurements. The variability of waves is followed by SWAN well. Results show that the wave height is overestimated by the model in all runs. r2 and r4 show slight improvement in the model results compare to r1 and r3. It is seen the best in the peak periods, with the increasing severity of weather condition. On 29.10.13 there is a unexpected peak in the model runs. It is not caused by meteorological forcing time steps as the wind is interpolate linearly on model time though the real reason is unknown.
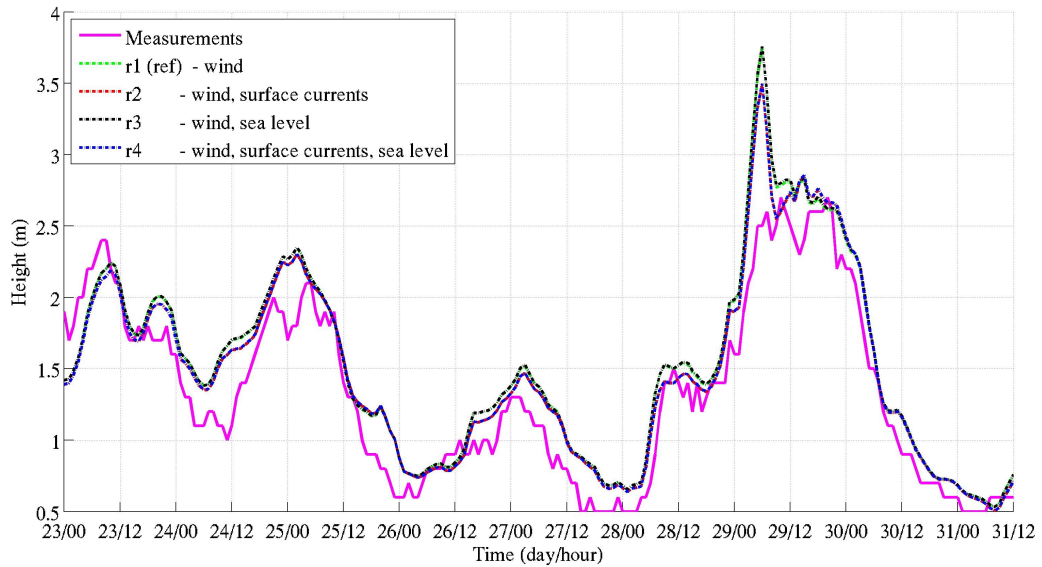
Figure 8. This is a figure of comparison of measurements of significant wave height taken in Gulf of Finland in station A and SWAN runs of r1 to r4

Next the statistical parameters for significant wave height are calculated using eq. 21–23 and presented in table 3. Calculated for the period of 23.10.13 00.00 to 31.10.13 23.00 (table 3. a) the best results are produced with r2 and r4, where surface currents are accounted. RMSE for reference run r1 is 28 cm, Scatter index 22 % and BIAS 19 cm. Taken into account currents (r2) RMSE decreases 3 cm, scatter index 3 % and BIAS 4 cm. Considering only sea level in the runs, has a negative effect on the results. This may be due to the fact that measurement point is situated in a deep water. The study of Alari (2013) shows that sea level plays more significant role in shallower waters.

Correlation between measurements and model is reasonably good 0.95 for all the runs.

Table 3 RMSE, Scatter index, BIAS and Correlation coefficient are calculated from comparison of measurements in Gulf of Finland (measurement station A, fig. 2) and model results. a) In time period from 23.10.13 00.00 to 31.10.13 23.00 – whole modelling period. Time period from 28.10.13 00.00 to 30.10.13 12.00 – during a storm on table b.

a)

23.10 00 - 31.10 23	RMSE (cm)	Scatter index (%)	BIAS (cm)	Correlation coefficient
Run 1	28	22	19	0.95
Run 2	25	19	15	0.95
Run 3	29	22	19	0.95
Run 4	25	19	16	0.95

b)

28.10 00- 30.10 12	RMSE (cm)	Scatter index (%)	BIAS (cm)	Correlation coefficient
Run 1	36	21	26	0.95
Run 2	29	17	21	0.96
Run 3	37	22	27	0.95
Run 4	30	18	21	0.96

Now looking to the statistics for the storm period 28.10 00.00 to 30.10 12.00 (table 3 b)). It is seen that accounting surface currents improves results has quite significant effect in storm conditions. As the RMSE of reference run r1 in storm conditions is 36 cm, it decreases when taking account currents 13 cm. Also scatter index and BIAS show improvement. Correlation goes from 0.95 (r1 and r3) to 0.96 (r2 and r4).

The time period for the validation in shallower water is from 26.10.13 to 31.10.12.

Measurements were taken close to Saaremaa Island by Estonian Marine Institute (Suursaar, 2013). The water depth at the measurement site was 5.5 m and the RDCP was bottom mounted . The measurement station is marked with B on fig. 2.

35

There was high-frequency cut-off and waves with period of 2.6 s and bigger were measured every hour. As a result the realistic significant wave height is bigger than measured. Measurements were taken in a location where depth differences were big in a small distance. On the model the closest point to measurement was in depth 21.10 m. Therefore another point in shallower water, with depth 7.83 m, was chosen.

On fig.9 it can be seen that, as in deeper water, model again overestimates measurements. Reference run r1 is closest to the measurement. Taking account currents (r2) increase the wave height. Considering sea level and also surface currents and sea level both increases the wave height even more. Gradually increasing significant wave height can be explained by the changes in the group velocity of waves. This is induced by surface currents and varying sea level. With a decrease in the group velocity there occurs decrease in the wave energy transport. In order to compensate that there is a increase in the wave energy density, which is reflected in the increase of the wave height.
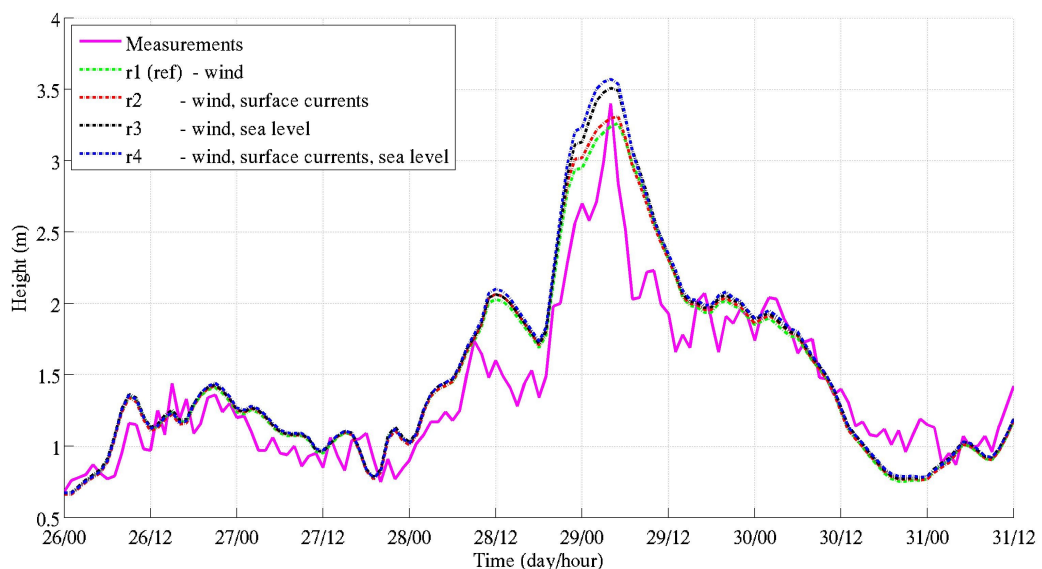
Figure 9. This is a figure of comparison of measurements of significant wave height taken close to Saaremaa in station B and SWAN runs of r1 to r4

Table 4 there is presented the statistical parameters. It is seen that errors are increasing as adding more dynamical forcings to the model. For example RMSE for the reference run r1 is 26 cm and for r4 it is 30 cm. This may be resulted in the fact that in shallow waters the bottom effects occur, making the relationship between wind, surface currents and sea level more complicated. There was a cut-off frequency in the measurements and a steep bottom slope in measurement station B. In addition the unknown local features may be the cause of increasing errors. Further on it is necessary to take measurement of waves and currents together in order to quantify the effect of currents on waves.

Table 4. This is a table of RMSE, Scatter index, BIAS and Correlation coefficient are calculated from comparison of measurements close to Saaremaa (measurement station B, fig. 2) and model result

STORM	RMSE (cm)	Scatter index (%)	BIAS (cm)	Correlation coefficient
Run 1	26	18	9	0.93
Run 2	27	19	10	0.93
Run 3	29	21	12	0.93
Run 4	30	22	13	0.94

From the validation it was seen that wave model SWAN produced the storm condition with good quality. In the time period of storm peak the difference between run r1 to r4 became most evident.

The quality of significant wave height produced by SWAN depends largely on the quality of input fields. HIRLAM wind fields has been assessed by Keevallik *et al.* (2010) and surface currents and sea level by Lagemaa (2012).

5.2 Spatial variability of the wave field

To see, how wave field is affected by the different dynamical forcings the maximum difference of significant wave height $\Delta m\, Hs^{n}$ and relative change $\Delta r\, Hs^{n}$ were found with with eq. 24 - 28. It was seen from the validations that effects are most noticeable in the peak periods. For this reason the day 29.10.13 was chosen to evaluate the spatial variability of the wave field.

On fig. 10 there is a probability density functions of spatial $\Delta m\, Hs^{n}$ distribution in a logarithmic scale. It shows the distribution of maximum difference of significant wave height. Also the probability that randomly picked point has according difference in the significant wave height.

With run r2 (red line), where wind and surface currents were present in the model there is a decrease in the wave height up to 50 cm and increase as big as 40 cm. There is present both decrease and increase in the wave height. When taking account wind and sea level (r3, black line) the difference is ranging from -10 to 100 cm. With varying sea level increase in the wave height is more evident. Accounting all the dynamical forcings wind, surface currents and sea level (r4, blue line) the difference of $\Delta m\, Hs^{4}$ can range from -50 to 100 cm. There is seen the joint effect that where $\Delta m\, Hs^{4}$ slightly grows and increase the distribution of positive increase in a range of 10 – 100 cm.
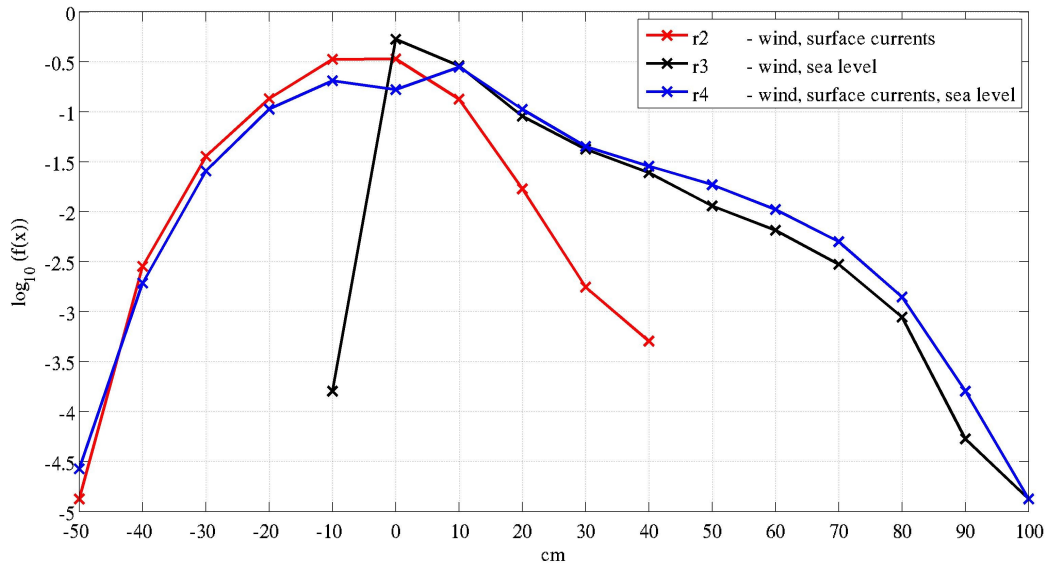
Figure 10. This is a figure of significant wave height maximum differences $\Delta m\,Hs^n$ probability in logarithmic scale for run r2, r3 and r4 on 29.10.13.

Next the maximum difference of significant wave height $\Delta m\,Hs^n$ are shown on fig. 12 on the left side and relative change $\Delta r\,Hs^n$ on the right side. The values shown are from -40 to 40 cm in maximum difference figures and from -20 to 20 % for the relative change to have a better visual overview.

On fig. 12 a and b there is the maximum difference and relative change in the significant wave height when taking account surface currents (r2). Increase in the wave height is most evident near the shore in a shallower water. In the southern part of Gulf of Finland near the shore there is an increase up to 10 cm (5 %). In in north-east of the Gulf of Riga there is an increase up to 20 cm (10-15 %). Near west shore of Hiiumaa wave height difference is about 10 to 20 cm (up to 20 %). In Saaremaa and in Irbe strait it can reach as high as 40 cm (up to 20 %). Near the small island in Gulf of Finland and Gulf of Riga there is a significant increase in the wave height. On fig. 11 every 10th vector of wave and current propagation direction at time

39

moment t^2_{max} are displayed. Wave directions are with black arrows and surface currents with blue arrows. As waves and surface currents are travelling more to the opposite directions, currents have a wave height increasing effect on waves. For example on fig. 11 in Pärnu bay, Irbe strait and west coast of the islands Hiiumaa and Saaremaa the waves and surface currents are propagating in the opposite directions. This results in a greater wave height increase, seen also in fig. 12 a and b.
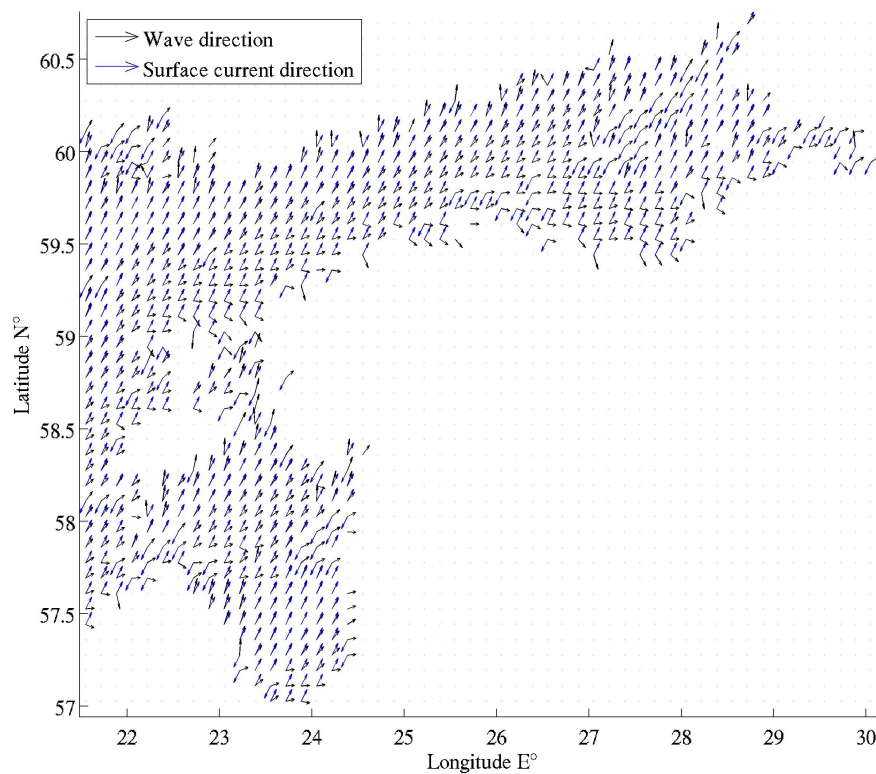
Figure 11. This is a figure of propagation directions for waves in run r2 and surface currents on the time moments of maximum differences on 29.10.13. Every 10 vector is displayed.

Decrease of the significant wave height occurs in deeper parts of the eastern Baltic Sea. In the Gulf of Riga and Gulf of Finland there is an decrease up to 15 cm (5 %). In Gulf of Finland between $25 - 26$ E^0 and $58.8 - 60$ N^0 wave height

decreases up 40 cm (20 %) (fig. 12 a and b). On fig. 11 it is seen that in these areas waves and surface currents are propagating more or less in the same direction and this results in a decrease of significant wave height, which is consistent also with the theory.

The maximum differences in significant wave height seem to occur in specific phase of the surface currents inertial oscillation. The magnitude in the increase and decrease of significant wave height is influenced by current velocity. For example in Irbe strait the current velocity reaches up to 195 cm s^{-1} (fig. 5) and from fig. 12 a and b it is seen that in this area the significant wave height is one of the most strongly affected areas by the surface currents.

On fig. 12 c and d there are presented the maximum difference and relative change of significant wave height when considering wind and sea level in the run (r3). In deeper parts of the eastern Baltic Sea, where the waves are not affected by the bottom, there is an increase in the significant wave height about 5 cm with relative increase of 5%. Near the shore, where the bottom effects come into play, there is noticeable a bigger increase in the wave height than in offshore. Irbe strait, west coast of Saaremaa, Hiiumaa and mainland of Estonia, in Pärnu bay, most westerly part of Gulf of Finland and in north shore of Gulf of Finland where the wave height increases most significantly. In these areas the maximum difference of significant wave height between reference run r1 and r3 is up to 40 cm (20 %). Also near shore of island in Gulf of Finland and Gulf of Riga there is a possible increase in the wave height of 40 %. It is seen that most significantly affected areas by the sea level are more exposed to the winds. This is also consistent with the work done by Alari (2013).

On fig. 12 e and f there is shown the joint effect of surface currents and sea level on the wave field. On wind open areas the total impact of surface currents and sea level impact on wave height increases. This was seen also from fig. 10. For example in Pärnu bay when accounting just currents the difference is up to 20 cm (10-15 %) the joint effect increases the wave height up to 40 cm (20 %). The spatial variability patterns of surface current effects and sea level both remain. Decrease in the significant wave height remained more or less in the same areas where it was when there was just surface currents present. In Gulf of Riga and Finland 15 cm (5 %), up to 40 cm (20 %).
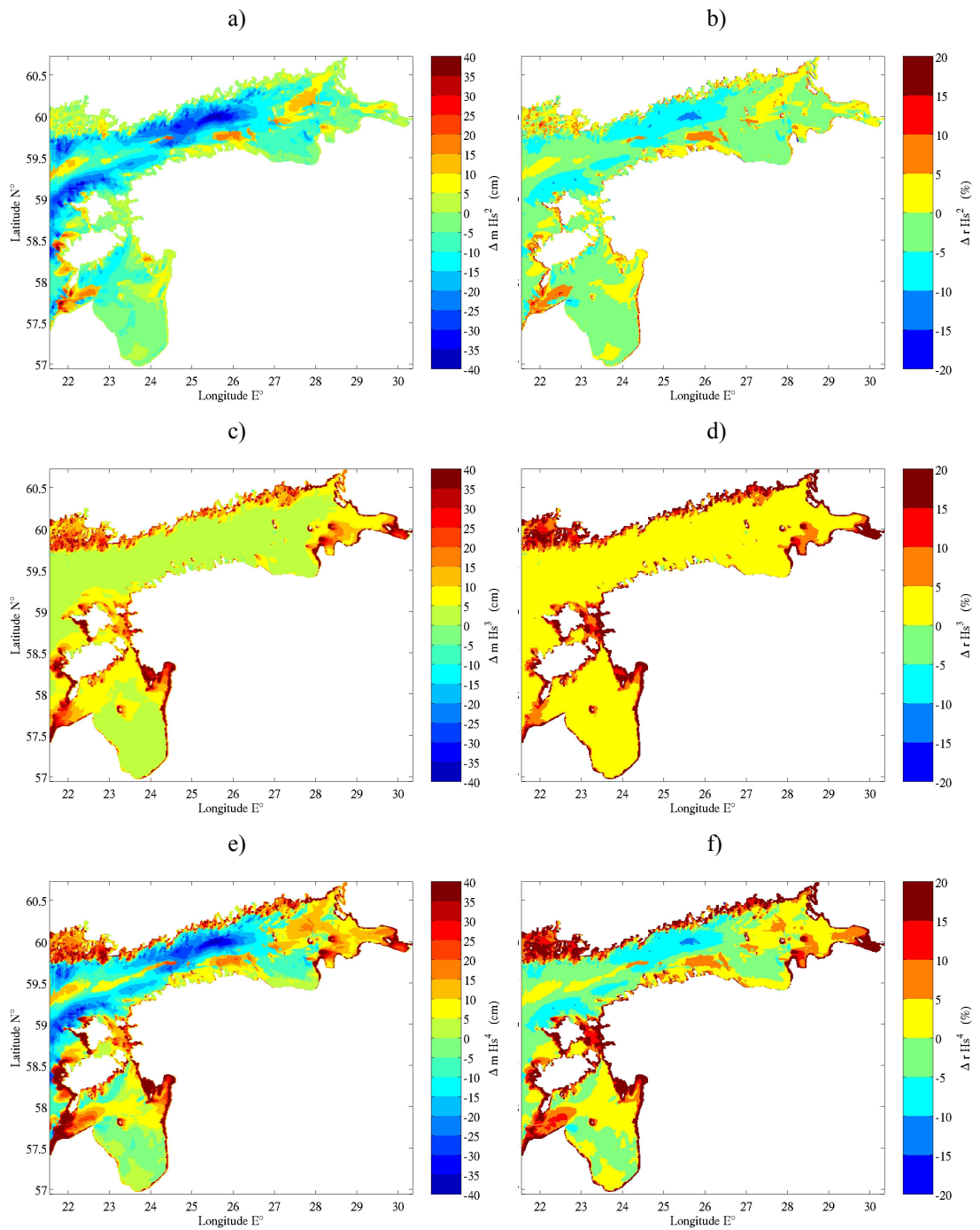
Figure 12. This is a figure of time maximum difference $\Delta m\, Hs^n$ and relative difference $\Delta r\, Hs^n$ in the significant wave height. a) and b) for r2, c) and d) for r3, e) and f) for r4. Values are in a range -40 to 40 cm and -20 to 20 % are shown on figure.

6. CONCLUSION

Thesis discussed wave-current interaction in horizontal dimension and as wave field development there was observed the total effect of physical phenomenas to the significant wave height.

It has two main objectives. Firstly, to see how surface currents and sea level effect significant wave height. Secondly, to study the spatial variability of surface currents and sea level effect on wave field. For this a hindcast of a storm St. Jude was modelled with wave model SWAN. Four runs (r1-r4, see table 2) with different dynamical forcings (wind, surface currents, sea level) were conducted.

- There was seen clear impact of surface currents and sea level to the significant wave height. Model overestimated the significant wave height but variations in the wave field were well simulated. Differences between runs r1 to r4 were best seen in peak periods.
- In deep water taking account surface currents improved the results, especially in storm conditions. Sea level was less significant.
- In shallower water the effect of sea level to the wave field evolution was more stronger than the surface currents. It was more noticeable in peak periods that surface currents and sea level gradually were increasing the significant wave height. This led to a distancing from the measurements. Accuracy in measurement and local topographic features may influence model validation.

- Different dynamical forcings produced the increase and decrease in the significant wave height in different ranges. With surface currents (r2) the decrease and increase was in a range of -50 to 40 cm. Sea level (r3) induced changes in a ranged of -10 to 100 cm. With joint effect of surface currents and sea level (r4) the range of increase and decrease was -50 to 100 cm.

- With surface currents taken account in the model (r2). Near the shore, where bottom started to effect the waves, there was more evident an increase in the significant wave height. In offshore occurred more a decrease in the wave height. This also depended on the directional spreading of waves and surface currents. With opposing currents there was an increase in the wave height and with following currents a decrease. The differences in significant wave height were more favourable by specific phase of the surface currents inertial oscillation. Magnitude of the difference was also impacted by the current velocity.

- Sea level (r3) produced stronger changes in the significant wave height near the shore in wind exposed areas.

- In wind open areas the combined effect of surface currents and sea level (r4) increased the wave height more. The spatial variability batters of surface currents and sea level remained.

- Surface currents and sea level both can induced changes in the significant wave height in a range of -20 % to 20 % near the shore

For further developments changes in the wave spectra, the influence of the propagation angles between currents and waves and interactions in the shallow water would give more knowledge about these interactions.

KOKKUVÕTE

Magistritöö uuris laine-hoovuse interaktsiooni horisontaalses dimensioonis ja laine evolutsioonil vaadeldi kogu füüsikaliste nähtuste mõju olulisele lainekõrgusele.

Seati kaks põhieesmärki. Esiteks, et näha kuidas pinnahoovused ja veetase mõjutavad olulist lainekõrgust. Teiseks, uuriti lainevälja ruumilist muutlikust pinnahoovuste ja veetaseme mõjul. Selleks modelleeriti SWAN mudeliga järelprognoos tormist St. Jude. Tehti neli arvutust (r1-r4, tabel 2) erinevate dünaamiliste mõjudega (tuul, pinnahoovused, veetase)

• Oli näha selge pinnahoovuste ja veetaseme mõju olulisele lainekõrgusele. Mudel ülehindas olulist lainekõrgust aga lainevälja muutlikus oli hästi tabatud. Erinevused arvutuste r1-r4 vahel tulid välja kõige paremini piigi ajahetkel.

• Sügavas vees, võttes arvesse pinnahoovuseid paranesid tulemused just tormi tingimustes. Veetase oli vähem oluline.

• Madalas vees veetaseme mõju lainevälja kujunemisele oli tugevam kui pinnahoovuste mõju. Piigi ajahetkel oli näha, et pinnahoovused ja veetase järk-järguliselt suurendasid olulist lainekõrgust. See viis mudeli tulemused eemale mõõtmistest. Mõõtmiste täpsus ja kohaliku topograafia eripärad võisid mõjutad valideerimi tulemusi.

- Erinevad dünaamilised mõjud põhjustasid olulise lainekõrguse kasvu ja kahanemise erinevates vahemikes. Pinnahoovused (r2) kasvatasid ja kahandasid lainekõrgust -50 kuni 40 cm. Veetase (r3) põhjustas muutusi vahemikus -10 kuni 100 cm. Pinnahoovuste ja veetaseme koosmõjul (r4) oli lainekõrguse kasv ja kahanemine vahemikus -50 kuni 100 cm.

- Võttes arvesse pinnahoovused (r2), ranna lähedal, kus põhi hakkas laineid mõjutama, oli tõenäolisem olulise lainekõrguse kasv. See sõltus ka lainete ja hoovuste levimise suundadest. Lainetuse ja pinnahoovuste vastassuunalisel levimisel toimus lainekõrguse kasv ja vastupidisel juhul lainekõrguse kahanemine. Maksimaalsed erienvused olulises lainekõrguses oli soodustatud teatud hoovuse inertsvõnkumise faasides ja mõjutatud ka hoovuse kiirustest.

- Veetase (r3) põhjustas tugevamaid muutusi olulises lainekõrguses ranna lähedal tuulele avatud aladel.

- Tuulele avatud aladel pinnahoovuste ja veetaseme koosmõju (r4) suurendas olulist lainekõrgust veelgi. Pinnahoovuste ja veetaseme ruumiliste muutlikuse mustrid säilisid.

- Pinnahoovused ja veetase, mõlemad olid võimelised põhjustama muutusi olulises lainekõguses vahemikus -20 % kuni 20 % ranna lähedal.

Edaspidi võiks uurida lainete-hoovuste-veetaseme interaktsiooni mõju laine spektile. Pinnahoovuste ja lainete vahelise nurga mõju ning interaktsioone madalas vees.

REFERENCES

Alari, V. (2013). Multi-Scale Wind Wave Modelling in the Baltic Sea. PhD dissertation, Tallinn University of Technology.

Alari, V., Raudsepp, U., Erm, A. (2010). Comparison of ADV measured near-bed orbital speed and latter derived from wave gauge measurements at intermediate water depths. In *Baltic International Symposium, 2010 IEEE/OES US/EU*. IEEE, 1-7.

Baltic Sea Hydrographic Commission. (2013). Baltic Sea Bathymetry Database version 0.9.3. Downloaded from http://data.bshc.pro/ on *21.03.2015.*

Battjes, J. A., (1994). Shallow water wave modelling. *Proc. Waves-Physical and Numerical Modelling*, University of British Columbia, Vancouver, 1-24

Battjes, J.A. J.P.F.M. Janssen. (1978). Energy loss and set-up due to breaking of random waves, *Proc. 16 th Int. Conf. Coastal Engineering*, ASCE, 569-587

Booij, N., Ris, R. C., Holthuijsen, L. H. (1999). A third-generation wave model for coastal regions: 1. Model description and validation. *Journal of Geophysical Research: Oceans (1978–2012)*, *104*(C4), 7649-7666.

Bretherton, F. P., Garrett, C. J. (1968). Wavetrains in inhomogeneous moving media. *Proceedings of the Royal Society of London. Series A. Mathematical and Physical Sciences*, *302*(1471), 529-554.

Burchard, H., Bolding, K. (2002). GETM: A General Estuarine Transport Model; Scientific Documentation. European Commission, Joint Research Centre, Institute for Environment and Sustainability.

Chawla, A., Kirby, J. T. (1998). Experimental study of wave breaking and blocking on opposing currents. *Coastal Engineering Proceedings*, *1*(26).

Dietrich, J. C., Dawson, C. N., Proft, J. M., Howard, M. T., Wells, G., Fleming, J. G., Luettich Jr., R.A., Westerink, J.J., Cobell, Z., Vitse, M., Lander, H.,Blanton, B. O., Szpilka, C. M., Atkinson, J. H. (2013). Real-time forecasting and visualization of hurricane waves and storm surge using SWAN+ ADCIRC and FigureGen. In *Computational Challenges in the Geosciences,* Springer, New York, 49-70

Feistel, R., Nausch, G., Wasmund, N. (2008). State and evolution of the Baltic Sea, 1952-2005: a detailed 50-year survey of meteorology and climate, physics, chemistry, biology, and marine environment. John Wiley & Sons, Hoboken.

Funkquist, L., Kleine, E. (2007). *HIROMB.* An introduction to HIROMB, an operational baroclinic model for the Baltic Sea. *Report oceanography No 37,* Swedish Meteorological and Hydrological Institute.

Hasselmann, K. (1974). On the spectral dissipation of ocean waves due to whitecapping. *Boundary-Layer Meteorology, 6 (1-2)*, 107-127.

Hasselmann, K., T.P. Barnett, E. Bouws, H. Carlson, D.E. Cartwright, K. Enke, J.A. Ewing, H. Gienapp, D.E. Hasselmann, P. Kruseman, A. Meerburg, P. M˙ Müller, D.J. Olbers, K. Richter, W. Sell and H. Walden. (1973). Measurements of wind−wave growth and swell decay during the Joint North Sea Wave Project (JONSWAP), Dtsch. Hydrogr. Z. Suppl., 12, A8

Haus, B. K. (2007). Surface current effects on the fetch-limited growth of wave energy. *Journal of Geophysical Research: Oceans (1978–2012), 112*(r3).

Holthuijsen, L. H. (2007). Waves in oceanic and coastal water. Cambridge University Press, New York, 404.

Huang, N. E., Chen, D. T., Tung, C. C., & Smith, J. R. (1972). Interactions between Steady Won-Uniform Currents and Gravity Waves with Applications for Current Measurements. *Journal of Physical Oceanography, 2*(4), 420-431.

Jaagus, J., Kull, A. (2011). Changes in surface wind directions in Estonia during 1966-2008 and their relationships with large-scale atmospheric circulation. *Estonian Journal of Earth Sciences*, *60*(4), 220-231.

Jonsson, I. G. (1990). Wave-current interactions. *The Sea, vol. 9, chapter 3*. New York: Wiley Interscience, 65-120.

Kahma, K. K. and Petterson, H. (1993). Wave statistics from the Gulf of Finland. *Finnish Institute of Marine Report*.

Keevallik, S., Männik, A., Hinnov, J. (2010). Comparison of HIRLAM wind data with measurements at Estonian coastal meteorological stations. *Estonian Journal of Earth Sciences,* 59(1), 90-99.

Lagemaa, P. (2012). Operational forecasting in Estonian marine waters. PhD dissertation, Tallinn University of Technology.

Liu, B., Ding, Y., Guan, C. (2007). A relationship between wave steepness and wave age for wind waves in deep water. *Chinese Journal of Oceanology and Limnology, 25*, 36-41.

Longuet-Higgins, M. S., Stewart, R. (1960). Changes in the form of short gravity waves on long waves and tidal currents. *Journal of Fluid Mechanics*, *8*(04), 565-583.

Longuet-Higgins, M. S., & Stewart, R. W. (1961). The changes in amplitude of short gravity waves on steady non-uniform currents. *Journal of Fluid Mechanics*, *10*(04), 529-549.

Longuet-Higgins, M. S., & Stewart, R. W. (1962). Radiation stress and mass transport in gravity waves, with application to 'surf beats'. *Journal of Fluid Mechanics*, *13*(04), 481-504.

Lonquet-Higgins, M. S., Stewart, R. W. (1964). Radiation Stress in water waves: a physical discussion with application. *Deep-Sea Research*, *11*, 529-562.

Luettich Jr, R. A., Westerink, J. J., Scheffner, N. W. (1992). ADCIRC: An Advanced Three-Dimensional Circulation Model for Shelves, Coasts, and Estuaries. Report 1. Theory and Methodology of ADCIRC-2DDI and ADCIRC-3DL (No. CERC-TR-DRP-92-6). Coastal Engineering Research Center Vicksburg MS.

MacIver, R. D., Simons, R. R., Thomas, G. P. (2006). Gravity waves interacting with a narrow jet-like current. *Journal of Geophysical Research: Oceans (1978–2012)*, *111*(r3).

Miles, J.W., (1957). On the generation of surface waves by shear flows, *J. Fluid Mech.*, 3, 185−204

Nwogu, O., (1993). Effect of Steady Currents on Directional Wave Spectra. *Proceedings of the 12th International Conference on Offshore Mechanics and Arctic Engineering* (OMAE), ASME, vol. 1, 25–32.

Phillips, O.M., (1957). On the generation of waves by turbulent wind, J. *Fluid Mech.*, 2, 417−445.

Phillips, O. M. (1977). The Dynamics of the Upper Ocean. 2nd edition, Cambridge University Press, New York, 336.

Raudsepp, U., Laanemets, J., Haran, G., Alari, V., Pavelson, J. and Kõuts, T. 2011. Flow, waves, and water exchange in the Suur Strait, Gulf of Riga, in 2008. *Oceanologia 53*: 35-56.

Ris, R. C., Holthuijsen, L. H. (1996). Spectral modelling of current induced wave-blocking. *Coastal Engineering Proceedings*, *1*(25).

Rosales, P., Ocampo-Torres, F. J., Osuna, P., Monbaliu, J., Padilla-Hernandez, R. (2008). Wave-current interaction in coastal waters: Effects on the bottom-shear stress. *Journal of marine systems*, *71*(1), 131-148.

Soares, C. G., de Pablo, H. (2006). Experimental study of the transformation of wave spectra by a uniform current. *Ocean engineering*, *33*(3), 293-310.

Soomere, T., Behrens, A., Tuomi, L. and Nielsen, J. W. 2008. Wave conditions in

the Baltic Proper and in the Gulf of Finland during windstorm Gudrun. *Natural Hazards and Earth System Sciences* 8: 37-46.

Soulsby, R. L., Hamm, L., Klopman, G., Myrhaug, D., Simons, R. R., Thomas, G. P. (1993). Wave-current interaction within and outside the bottom boundary layer. *Coastal engineering*, *21*(1), 41-69.

Suursaar, Ü (2013). Locally calibrated wave hindcasts in the Estonian coastal sea in 1966–2011. *Estonian Journal of Earth Sciences,* 62(1), 42 – 56.

Suursaar, Ü., Kullas, T. and Aps, R. 2012. Currents and waves in the northern Gulf of Riga: measurements and long-term hindcast. *Oceanologia,* 54, 421-447

The SWAN team. (2013a). SWAN: Scientific and technical documentation. *Cycle III version 40.91.* Delft University of Technology, Department of Civil Engineering, the Netherlands.

The SWAN team. (2013b). SWAN: User manual. *Cycle III version 40.91.* Delft University of Technology, Department of Civil Engineering, the Netherlands.

The WAMDI Group. (1988). The WAM model-a third generation ocean wave prediction model. *Journal of Physical Oceanography*, *18*(12), 1775-1810.

Thomson, R. E. (1981). Oceanography of the British Columbia coast (No. 56). Gordon Soules Book Pub.

Tolman, H. L. (2009). User manual and system documentation of WAVEWATCH III TM version 3.14. *Technical note, MMAB Contribution*, *276*.

Unden, P., Rontu, L., Jarvinen, H., Lynch, P., Calvo, J., Cats, G., Cuxart, J., Eerola, K., Fortelius, C., Garcia-Moya, J.A., Jones, C., Lenderlink, G., McDonald, A., McGrath, R., Navascues, B., Nielsen, N.W., Odegaard, V., Rodriguez, E., Rummukainen, M., Rõõm, R., Sattler, K., Sass, B.H., Savijarvi, H., Schreur, B.W., Sigg, R., The, H., Tijm, A. (2002). HIRLAM-5 scientific documentation. Swedish Meteorological and Hydrological Institute, Sweden.

van der Westhuysen, A. J. (2012). Spectral modeling of wave dissipation on negative current gradients. *Coastal Engineering*, *68*, 17-30.

Van der Westhuysen, A. (2012). Modeling nearshore wave processes. In *ECWMF Workshop on "Ocean Waves", European Centre for medium-range weather forecasts, Reading*.

Whitman, G. B. (1974). Linear and nonlinear waves. *J. Wiley, New York*.

Wolf, J., Prandle, D. (1999). Some observations of wave–current interaction. *Coastal Engineering*, *37*(3), 471-485.